

# Reliable decoding of motor state transitions during imagined movement

B. Orset\*, K. Lee\*, R. Chavarriaga\* and J. d. R. Millán\*, Fellow, IEEE

**Abstract** – Current non-invasive Brain Machine interfaces commonly rely on the decoding of sustained motor imagery activity. This approach enables a user to control brain-actuated devices by triggering predetermined motor actions. However, despite of its broad range of applications, this paradigm has failed so far to allow a natural and reliable control. As an alternative approach, we investigated the decoding of states transitions of an imagined movement, i.e. rest-to-movement (onset) and movement-to-rest (offset). We show that both transitions can be reliably decoded with accuracies of 71.47% for the onset and 73.31% for the offset (N = 9 subjects). Importantly, these transitions exhibit different neural patterns and need to be decoded independently. Our results indicate that both decoders are able to capture the brain dynamics during imagined movements and that their combined use could provide benefits in terms of accuracy and time precision.

## I. INTRODUCTION

Brain Machine Interface (BMI) enables users to bypass conventional communication and control pathways, conveying messages and commands to the external world through brain-actuated devices. For motor tasks, most non-invasive BMIs aim to detect the onset of a movement which is then used to trigger predefined motor actions. Indeed, the output of a BMI decoder is usually coupled with an effector that can assist and translate the user intention into a motor command. Although the detection of imagined movement onset is critical in the process [1, 2], decoding the volitional interruption of a motor attempt is of equally importance in order to endow brain-actuated devices with more natural behavior. However, the decoding of the action offset has been barely investigated in the BMI field.

One main property of the brain is the ability of neurons to work in synchrony and to generate oscillatory activity [3]. It is known that changes in the brain rhythms during motor imagery (MI) can be recorded and decoded non-invasively through electroencephalogram (EEG). During motor imagery, a decrease of power (event-related desynchronization, ERD) can be observed in  $\mu$  band (8-12 Hz) as well as in  $\beta$  band (13-25 Hz) over the contralateral sensorimotor cortex. On the opposite, an increase of power

(event-related synchronization, ERS) in the  $\beta$  band (known as the  $\beta$  rebound) is induced after movement termination [4, 5]. Such synchronization can last for a second and can also be observed after MI [4]. Although the role of  $\beta$  rebound is still under debate, it is thought to have a functional role of inhibition of the motor cortex by somatosensory processing [5, 6] or could reflect an active process to promote existing motor set aiming to maintain current sensorimotor or cognitive state (i.e. status quo) [7]. Similarly, the presence of  $\alpha$  ERS was also reported and could be explained as an electrophysiological correlate of cortical idling state [8].

In this study, we investigated the different motor state transitions of an imagined movement, i.e. rest-to-movement (onset) and movement-to-rest (offset). Results reveal that these state transitions can be decoded independently with high reliability by exploiting their distinct neural correlates.

## II. METHODS

### A. Protocol

Nine healthy naïve subjects (19-26 years, 4 women) participated in this experiment. Participants were asked to perform kinesthetic MI (i.e. imagine the feeling associated with performing a movement) of both hands simultaneously. The duration of MI task was varying for each trial between 2 and 4 s and was cued using a clock hand (Fig. 1). During the trial, the participant was asked to continuously look at a fixation cross located in the middle of a clock. The participant was instructed to avoid blinks and muscular contractions. At the beginning of a trial, the participant was in a rest state during 3 s. Then, the clock hand started to move (cued-MI initiation) indicating to perform MI until it reached a target indicated with a red bar (cue-based termination). After MI termination (MI<sub>t</sub>), subjects were instructed to stay calm avoiding any muscular contraction or blinks. In between trials, a relaxation phase allowed the participant to blink and move during 7 s. The structure of the trial is illustrated in Fig. 1. Each subject was asked to perform 4 runs of 30 trials (120 trials in total).

### B. Recording System

EEG signals were acquired with a 16-channel g.USBamp amplifier (g.Tec medical engineering, Schiedelberg, Austria) at a sampling rate of 512 Hz. EEG electrodes were placed over

\*Research supported by the Swiss NCCR Robotics.

The authors are with the Defitech Chair in Brain Machine Interface, Center for Neuroprosthetics, Ecole Polytechnique Fédérale de Lausanne, Geneva, Switzerland (e-mail: bastien.orset@epfl.ch).

the sensorimotor cortex according to the international 10–10 system. The amplifier was set with a hardware band-pass frequency between 0.01 and 100 Hz (Butterworth 4<sup>th</sup> order) and a notch filter between 48 Hz and 52 Hz. A Common Average Reference was used on the EEG raw data filter to enhance the Signal-to-Noise Ratio.

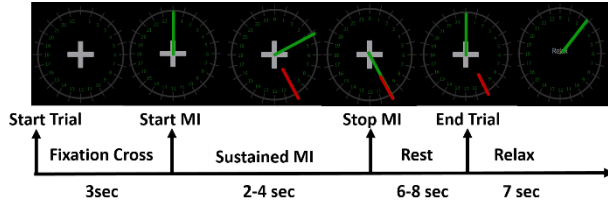


Figure 1. Trial structure. During a trial, the subject is asked to continuously look at a fixation cross in the center of the clock. The subject is instructed to stay calm during the first 3 seconds without moving or blinking. A clock hand (green bar) indicates to the subject to initiate his motor imagery of both hands. When the clock hand reaches a target (red bar), the subject stops motor imagery and stays at rest (no blink or movement). A period of 7 seconds following each trial allows the subject to relax.

### C. Features extraction and classification

To detect the onset and offset transitions, power spectral densities were computed in a 1s-window using the Welch’s method (0.5 s window with 0.25 s non-overlapping window) from 4 to 40 Hz with a 2 Hz resolution on the 16 channels. In total, 304 features were generated. A 10-fold trial-based cross-validation was performed where the 6 best features from each fold were selected based on their Fisher Score. Using these features, a Diagonal Linear Discriminant Analysis (DLDA) was trained. Feature vectors were obtained from each sample in the training dataset and z-score normalized. Their mean and variance were applied on the feature vectors in the testing dataset. To test whether the decoding performances were above chance, we estimated the statistical chance threshold at the 95% confidence interval based on the inverse binomial cumulative distribution (uniform priors,  $n = 408$  samples in test set), leading to a value of 54.17%. All the presented analysis was performed offline.

**Onset decoding:** An onset decoder was trained to distinguish between sustained MI characterized by the presence of ERD

and rest state (REST). 1-second long samples were computed with a sliding window of 62.5 ms in the time intervals  $[0, 2]$  s (MI class) and  $[-2, 0]$  s (REST class) with respect to the onset. A total of 17 samples were collected per trial for each class.

**Offset decoding:** An offset decoder was trained to distinguish between sustained MI and MI<sub>t</sub> with the later characterized by the presence of ERS. 1-second long samples were computed with a sliding window of 62.5 ms in the time intervals  $[-2, 0]$  s (MI) and  $[0.5, 2.5]$  s (MI<sub>t</sub>) with respect to the offset. A total of 17 samples were collected per trial for each class.

### D. Classification performances

To assess the performances of both classifiers, we calculated the accuracy at the sample level over the 10-fold cross validation. The accuracy was defined as the number of correctly classified samples over the total number of samples and was computed for each fold. Additionally, a pseudo-online analysis was performed to study classifier behavior in real-time at the trial level. In this analysis, both classifiers were tested in the time interval  $[-3, 4]$  s with respect to the onset. During this time interval, the likelihood (i.e. the probability to detect MI) was calculated from both decoders on samples computed with a 1s-buffer shifted every 62.5ms. A similar analysis was performed with respect to the offset where the likelihood was defined as the probability to detect MI<sub>t</sub>.

## III. RESULTS

### A. Time frequency analysis

A spectral analysis was first performed on central channels where we evaluated the event-related spectral changes for onset and offset. Fig. 2 shows the grand averages across subjects. During sustained MI, an ERD in both  $\mu$  and  $\beta$  bands could be observed more prominently on centro-lateral channels (C3, C4). On the opposite, an ERS in upper  $\mu$  band (11-13 Hz) was seen on these channels around 1s after MI termination. An ERS was also observed in  $\beta$  band in C3 and C4 but was less prominent due to inter-subject variability. Interestingly, the ERS tends to last longer in the upper  $\mu$  band than in the  $\beta$  band.

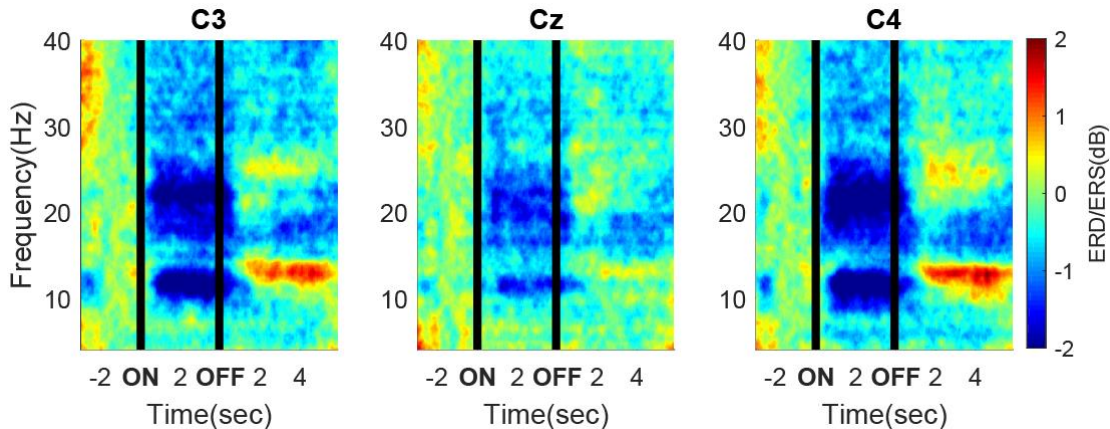


Figure 2. Grand average spectrogram on central channels across subjects and averaged over all trials. The first vertical line corresponds to the onset (ON) where the participant initiates his motor imagery while the second one is the offset (OFF) and corresponds to the time when she stopped.

## B. Decoding performance

We evaluated the performances of both onset and offset decoders. Fig. 3 shows the accuracy of the decoders for each subject and in grand average. On one hand, when decoding the onset, an offline average accuracy was achieved at the sample-based level of  $71.47\% \pm 6.01\%$  (mean  $\pm$  std). On the other hand, in the case of the offset, an average accuracy of  $73.31\% \pm 6.96\%$  (mean  $\pm$  std) was obtained. Importantly, both classifiers decode above the statistical chance threshold (54.17%) for every subject (except s3 for offset decoding). Additionally, Fig. 4 shows the Fisher scores of the spectral features averaged over the different folds of the cross validation and subjects for both classifiers. Note that for both decoders, most information can be found in  $\mu$  and  $\beta$  bands on central channels located over the hand motor area. Although similar channels were found informative, higher fisher scores were observed in the case of the offset decoder. This is because of the decoding approach chosen to detect each transition where the pre-transition time is compared with the post-transition time. Therefore, the onset decoder distinguishes neural correlates of MI initiation (ERD) from a controlled state (REST) while the offset decoder differentiates neural correlates of initiation (ERD) from neural correlates of termination (ERS).

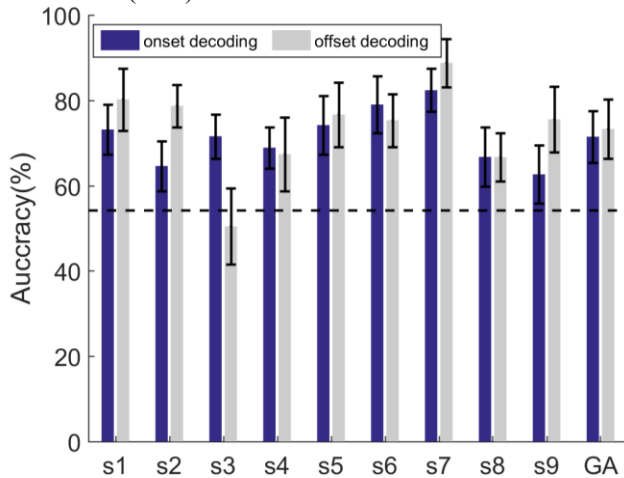


Figure 3. Accuracy of onset and offset decoders at the sample level. Accuracy is reported for every subject (s1-s9) as well as in grand average (GA). The standard deviation is shown on each bar. The statistical chance threshold (54.17%) is represented with a dash line.

To study the behavior of each classifier during both transitions, we performed a pseudo-online analysis where we applied the onset classifier as well as the offset classifier on the same time interval. To be able to compare, labels “MI” were switched into “REST” during the offset transition for the onset decoder; conversely, “REST” samples were relabeled as “MI” during the onset transition. Fig. 5a and Fig. 5b report the grand-average results over the nine subjects of the pseudo-online analysis on the onset and the offset transitions, respectively. During the pre-onset period (Fig. 5a), the offset decoder outputs a higher likelihood than that of the onset decoder and with values close to chance level (0.5) meaning that the offset decoder is not able to classify the rest state accurately. Additionally, we can notice that the standard

deviation of the likelihood is also bigger in the case of the offset decoding. On the opposite, during the pre-offset period (Fig. 5b), the onset decoder shows a smaller likelihood to detect MI while after the offset, its likelihood shows a sharper increase and reach a higher value. A smaller standard deviation is also observed for the offset decoder.

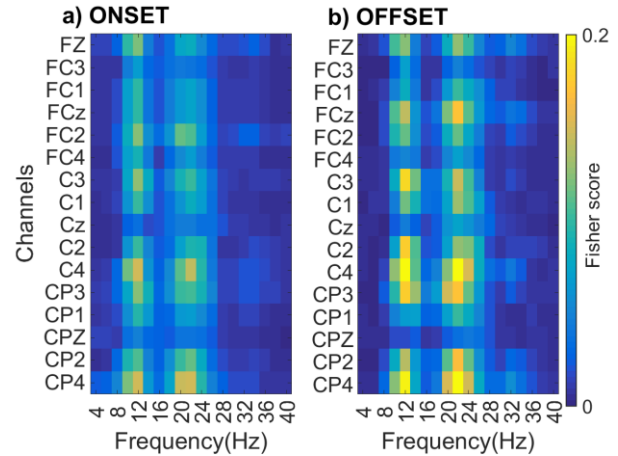


Figure 4. Fisher score map averaged over subjects for the onset and offset classifiers. The map of the onset classifier is shown in left (a) while the map of the offset classifier is shown on the right (b). Fisher scores are shown for the combinations of channels x frequencies. A color close to yellow indicates highly informative features while a blue one indicates irrelevant features.

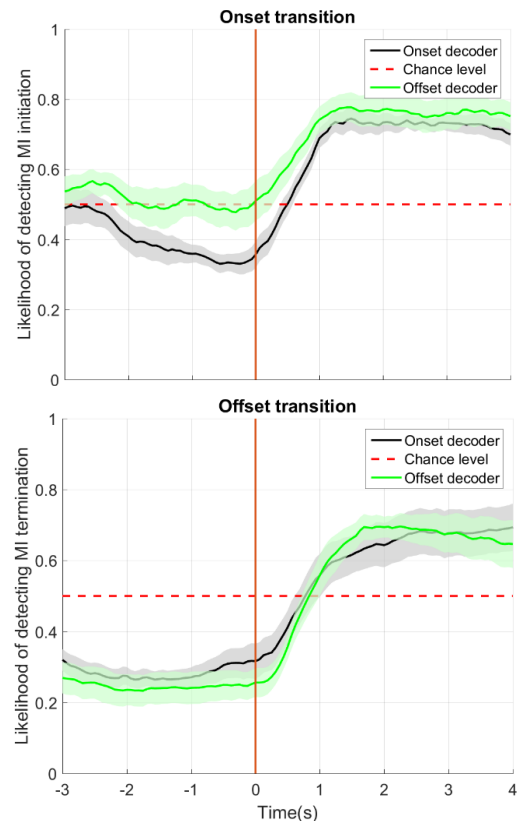


Figure 5. Grand-average pseudo-online decoding of onset and offset MI (N = 9). The likelihood of both decoders is shown over time. a) Pseudo-online decoding applied on the initiation transition ( $t=0$ ) of MI. b) Pseudo-online decoding applied on the termination transition ( $t=0$ ) of MI. The offset decoder is represented in green and the onset decoder is represented in black. The standard deviation is shown at every time point. The chance level is represented in red.

## IV. DISCUSSION

### A. Time Frequency Analysis

From the spectral analysis performed, neural correlates of motor termination were identified and are consistent with the literature [4, 5, 6, 8]. These correlates are characterized by an increase of power in the upper  $\mu$  and  $\beta$  bands. They are localized over the sensorimotor cortex reinforcing their role in the termination of an imagined motor action. Interestingly, it appears that the  $\mu$  ERS seems to be more present and reliable than the  $\beta$  ERS. More importantly, this ERS tends to last longer in the  $\mu$  band than in the  $\beta$  band, which facilitates its detection.

### B. Decoding Performances

A previous study has shown the feasibility to decode both transitions independently [9]. This was done when performing brisk foot MI distinguishing a rest state from either ERD or ERS. Compared to our study, two main differences can be observed. First, our protocol requires that the participant performs sustained MI instead of brisk MI. Thus, our results suggest that offset correlates cannot only be used when performing brisk activity but also for sustained activity which is more commonly used in BMI. Second, the decoding approach was different from ours as we relied on the specific neural correlates of each transition, comparing the time before the transition and the time after the transition. Indeed, when training our model for detecting MI initiation our decoder tries to distinguish REST from ERD, while the offset decoder was trained to differentiate between ERD and ERS. This implies that, theoretically, the offset decoder should yield higher performance because the difference of band power amplitude between ERD and ERS is much stronger than the one between ERD and the rest state [10]. Our results seem to corroborate this hypothesis since in grand average the offset decoding tends to provide higher performances than onset decoding. Also, most of the subjects ( $n = 5$ ) tends to have higher accuracies in the case of the offset decoding. Additionally, Fisher scores maps reveal that features are more discriminant in the case of the offset decoder.

### C. Decoding behavior

Most MI-based BMI studies aim to detect MI as a sustained activity. However, here we provide arguments for a different approach based on the decoding of motor state transitions that may bring a benefit in terms of accuracy and time precision. When comparing the behavior of both decoders in a pseudo-online analysis, we can conclude that the onset decoder is more suitable to detect MI initiation since the offset decoder is not able to capture the rest state. However, when decoding MI termination, it is more difficult to identify which decoder should be used for this transition since both decoders show a similar behavior. Nevertheless, our results suggest that using the offset decoder could be more suitable to use than the onset decoder to detect the termination of an imagined movement.

## V. CONCLUSION

In this paper, we have shown that the different transitions of an imagined movement can be decoded independently. These

transitions exhibit different neural correlates that can be exploited to ensure a reliable decoding. Both decoders show similar features although they tend to be more discriminant during offset decoding. Importantly, our results highlight that each transition should be decoded by a specific model in order to capture the whole dynamic of an imagined movement. Based on these results, the next stage of our research aims to combine both decoders using a finite-state machine model. Indeed, we believe that the decoding of these two transitions could help us to reach asynchronous control and improve the reliability of our neuroprostheses. We are currently running a study to probe our hypothesis.

## REFERENCES

- [1] I. K. Niazi, N. Jiang, and O. Tiberghien, "Detection of movement intention from single-trial movement-related cortical," *J. Neural Eng.*, vol. 66009, no. 8, pp. 1–10, 2011.
- [2] E. Lew, R. Chavarriaga, S. Silvoni, and J. d. R. Millán, "Detection of self-paced reaching movement intention from EEG signals," *Front. Neuroeng.*, vol. 5, 2012.
- [3] H. Jasper and W. Penfield, "Electrocorticograms in man: effect of voluntary movement upon the electrical activity of the precentral gyrus," *Archiv für Psychiatrie und Nervenkrankheiten*, vol. 183, no. 1-2, pp. 163–174, 1949.
- [4] G. Pfurtscheller, C. Neuper, K. Pichler-Zalaudek, G. Edlinger, and F. H. Lopes Da Silva, "Do brain oscillations of different frequencies indicate interaction between cortical areas in humans?," *Neurosci. Lett.*, vol. 286, no. 1, pp. 66–68, 2000.
- [5] E. Houdayer, E. Labyt, F. Cassim, J. L. Bourriez, and P. Derambure, "Relationship between event-related beta synchronization and afferent inputs: Analysis of finger movement and peripheral nerve stimulations," *Clin. Neurophysiol.*, vol. 117, no. 3, pp. 628–636, 2006.
- [6] F. Cassim *et al.*, "Does post-movement beta synchronization reflect an idling motor cortex?," *Neuroreport*, vol. 12, no. 17, pp. 3859–3863, 2001.
- [7] A. K. Engel and P. Fries, "Beta-band oscillations-signalling the status quo?," *Curr. Opin. Neurobiol.*, vol. 20, no. 2, pp. 156–165, 2010.
- [8] G. Pfurtscheller, A. Stancák, and C. Neuper, "Event-related synchronization (ERS) in the alpha band - An electrophysiological correlate of cortical idling: A review," *Int. J. Psychophysiol.*, vol. 24, no. 1–2, pp. 39–46, 1996.
- [9] G. Pfurtscheller and T. Solis-Escalante, "Could the beta rebound in the EEG be suitable to realize a 'brain switch'?", *Clin. Neurophysiol.*, vol. 120, no. 1, pp. 24–29, 2009.
- [10] A. Stancák and G. Pfurtscheller, "Event-related desynchronization of central beta-rhythms during brisk and slow self-paced finger movements of dominant and nondominant hand," *Cogn. Brain Res.*, vol. 4, no. 3, pp. 171–183, 1996.